Deep Red (DR) to Near Infrared (NIR) Light Controlled Ruthenium Catalyzed Olefin Metathesis

David C. Cabanero,[1] Jennifer A. Nguyen,[1] Catherine S. J. Cazin,[2] Steven P. Nolan,[2] Tomislav Rovis*[1]

[1]Department of Chemistry, Columbia University, New York, NY, 10027, United States

[2]Department of Chemistry and Center for Sustainable Chemistry, Ghent University, Krijgslaan 281, S3, Ghent, 9000 Belgium.

Keywords: Catalysts, Photocatalysis, Light, Irradiation, Metathesis

ABSTRACT: A system has been developed to activate a latent ruthenium olefin metathesis catalyst using deep red to near infrared light (600-800 nm) in conjunction with an osmium (II) photocatalyst that is directly excited to its triplet state via spin-forbidden excitation. An excited state single electron reduction of a latent solvent coordinated, cationic pre-catalyst is proposed as the operating mechanism for activation and photocontrol, as probed via *in situ* LED NMR kinetic studies and cyclic voltammetry. Excellent levels of spatiotemporal control are found under light irradiation. NIR olefin metathesis exhibits improved light penetration through barriers over shorter wavelengths of light, a control element that was deployed to mold dicyclopentadiene via ROMP.

INTRODUCTION

Olefin metathesis is one of the most attractive transformations in the synthetic chemist's arsenal, forming a carbon-carbon double bond with high efficiency under exceedingly mild, functional group tolerant conditions. Indeed, this reaction has deeply impacted synthetic organic chemistry[1-4], materials and polymer science.[5,6] With the prospect of controlling metathesis and its mechanistic congeners with high levels of spatial and temporal control, interest in activating latent metathesis catalysts is steadily growing.[7,8] For instance, Ring Opening Metathesis Polymerization (ROMP) is highly robust and creates mechanically strong polymers; however, its temporal control is still an ongoing challenge. Examples of controlling ROMP through different stimuli have emerged, including electro-[9–11], mechano-[12], and photochemistry.[13–18] Of these, the use of light is highly attractive as it is a mild mode of activation while enabling precise spatial control with high resolution through lasers, and excellent temporal control with the simple flip of the switch.

Several methods have been used to photoactivate latent Ru complexes, such as by activating various benzylidene complexes via UV to visible light or generation of photoacids.[14-16] Metal-free ROMP has been developed using a photocatalyst to oxidize enol ethers.[17] We have previously described a bis-*N*-heterocyclic carbene (NHC) coordinated Ru complex which when treated with blue light in the presence of an oxidizing photocatalyst leads to light-controlled olefin metathesis.[18] Herein, we demonstrate the exquisite control of olefin metathesis via Deep Red (DR) to Near-Infrared (NIR) photoredox catalysis. This system not only offers full spatiotemporal control for the catalyzed metathesis reaction, but also provides all advantages of NIR light over blue light regarding barrier penetration, allowing new ways to mold polymers.

With our previous blue light system, a highly oxidizing photocatalyst (PC*/PC$^{\bullet+}$ = +2.55 V) was used to dissociate the strongly bound IMes ligand (Scheme 1) from the metal center.

Scheme 1: Recent Work on Photo-Controlled Olefin Metathesis

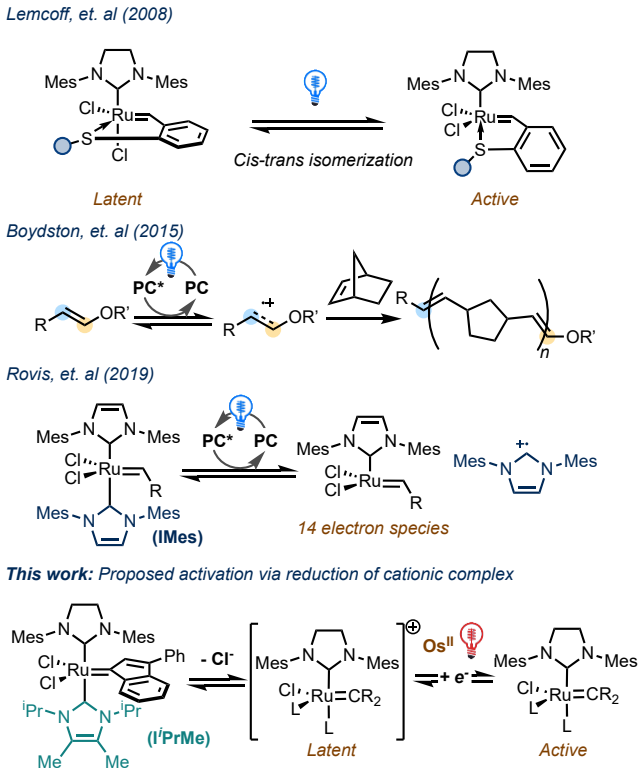

Since the lability of the NHC ligand is critical, we sought more easily activated, latent complexes. A set of mixed bis-NHC phenylindenylidene catalysts that contain a SIMes ligand *trans* to a smaller, more labile NHC ligand has been previously reported and successfully used by the Nolan group with low catalyst loadings (0.02 mol%).[19] However, it was found that a derivative containing an I^{i}PrMe NHC ligand did not perform well under

thermal conditions.

This latent I^{i}PrMe precatalyst may be susceptible to milder, DR to NIR photoredox activation since the I^{i}PrMe is more labile compared to the IMes ligand from our previous work. To achieve this low energy light activation, we use our recently described set of Os(II) polypyridyl complexes,[20] which are known to proceed through direct S_0-T_1 excitation and we recently used in metallaphotoreox chemistry.[21] This spin-forbidden excitation occurs for these Os complexes as they possess stronger spin-orbit coupling (SOC) than their Ru counterparts (such as [Ru(bpy)$_3$]) by virtue of the heavy atom effect. Thus, transitions governed by SOC such as intersystem crossing and direct S_0-T_1 excitation are greatly influenced by simply modifying the metal center to a heavier atom. The Os(II) polypyridyl ^{3}MLCT band is directly observed through UV-Vis spectroscopy, typically appearing in the 600-800 nm (DR to NIR-I) range. As such, we take advantage of this strong SOC by virtue of this heavy atom effect, directly excite these complexes to their triplet excited states, and perform valuable organic transformations with low energy, highly penetrating light.

RESULTS AND DISCUSSION

Table 1: RCM optimization and scope.

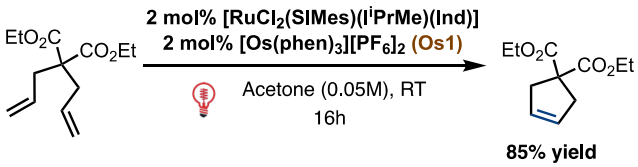

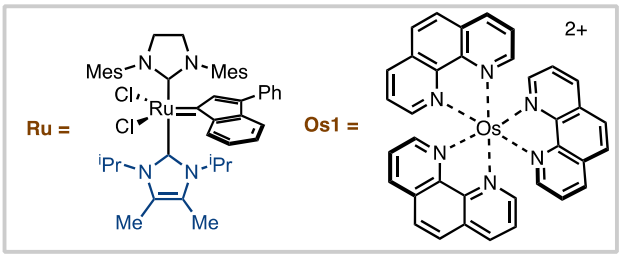

Entry	Conditions	Yield[a]
1	1 mol% Os1, 0.2 M	22
2	1 mol% Os1, 0.1 M	41
3	1 mol% Os1, 0.05 M	73
4	**2 mol% Os1, 0.05 M**	**85**
5	2 mol% Os1, 0.05 M, **no light**	trace
6	Ru only, 0.05 M, **light**	trace
7	Ru only, 0.05 M, **no light**	trace

Ring Closing Metathesis[b]

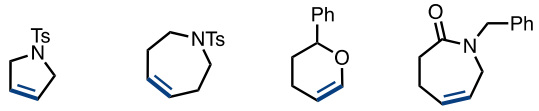

85% 84% 37% 66%

[a] ^{1}H-NMR yield with 1,3,5-trimethoxybenzene as internal standard.
[b] Isolated yields.

The ring closing metathesis (RCM) of diethyl diallylmalonate using this I^{i}PrMe derivative and [Os(phen)$_3$][PF6]$_2$ (**Os1**) as photocatalyst is achieved in up to 85% yield, where the yield increases with decreased concentration (Table 1). Acetone is used as a coordinating solvent, which also provides a polar environment, a factor that will be discussed in the mechanistic analysis. Trace amounts (<2%) are observed without light, without the Os photocatalyst, and without both. The RCM of several typical substrates to make 5-7 membered rings proceeds in 37-85% yield. Likewise, ROMP of 1,5-cyclooctadiene and norbornene is achieved with >95% conversion within one hour.

Table 2: Photocatalyst and additive screens.

a. Photocatalyst screen

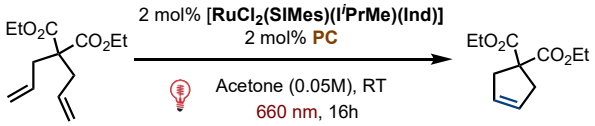

Entry	Photocatalyst	T_1 (kcal/mol)	Os^{II*}/Os^{III}	% Yield[a]
1	**Os1**	**44.1**	**-0.93**	**85**
2	Os2	42.5	-0.86	76
3	Os3	42.2	-0.75	63
4	Os4	41.3	-0.70	11
5	Os5	40.6	-0.62	2

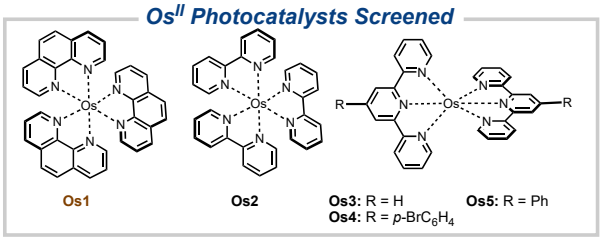

b. Additive screen

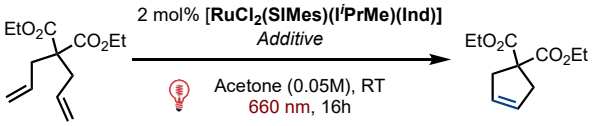

Entry	Additive	Light	Time	% Yield[a]
1	1 equiv. Zn	no light	16h	34%
2	20 mol% nBu_4NPF_6	660 nm	16h	trace
3	20 mol% nBu_4NPF_6	no light	16h	trace
4	**2 mol% Os1**	660 nm	4h	14%
5	**2 mol% Os1** 20 mol% nBu_4NPF_6	660 nm	4h	25%
6	**2 mol% Os1** 10 mol% I^{i}PrMe	660 nm	16h	**NR**

[a] ^{1}H-NMR yield with mesitylene as internal standard

The salient finding here is not the ability to ring-close diallylmalonate but the control exerted by DR light. With this in mind, we turned our attention to elucidating the mechanism of

activation, with the intent to showcase the enabling features afforded by DR activation. In contrast to our previous oxidative blue light system,[18] the yield in the DR controlled system increases as Os^{II}*/Os^{III} decreases (a better *reducing agent* in the excited state), despite the photocatalysts having similar triplet energies, T_1 (Table 2a). For example, **Os2** (Table 2a, entry 2) and **Os4** (Table 2a, entry 4) have triplet energies within approximately 1 kcal/mol of each other but deliver significantly different yields. Furthermore, the lack of spectral overlap between the Ru absorption and Os emission spectra suggests that an energy transfer mechanism is unlikely (SI Figure S5). Meanwhile, using Zn as a stoichiometric reductant provides 34% yield (Table 2b, entry 1), which suggests that the mechanism to precatalyst activation could indeed proceed through a reductive pathway.

Scheme 2: Mechanistic analysis

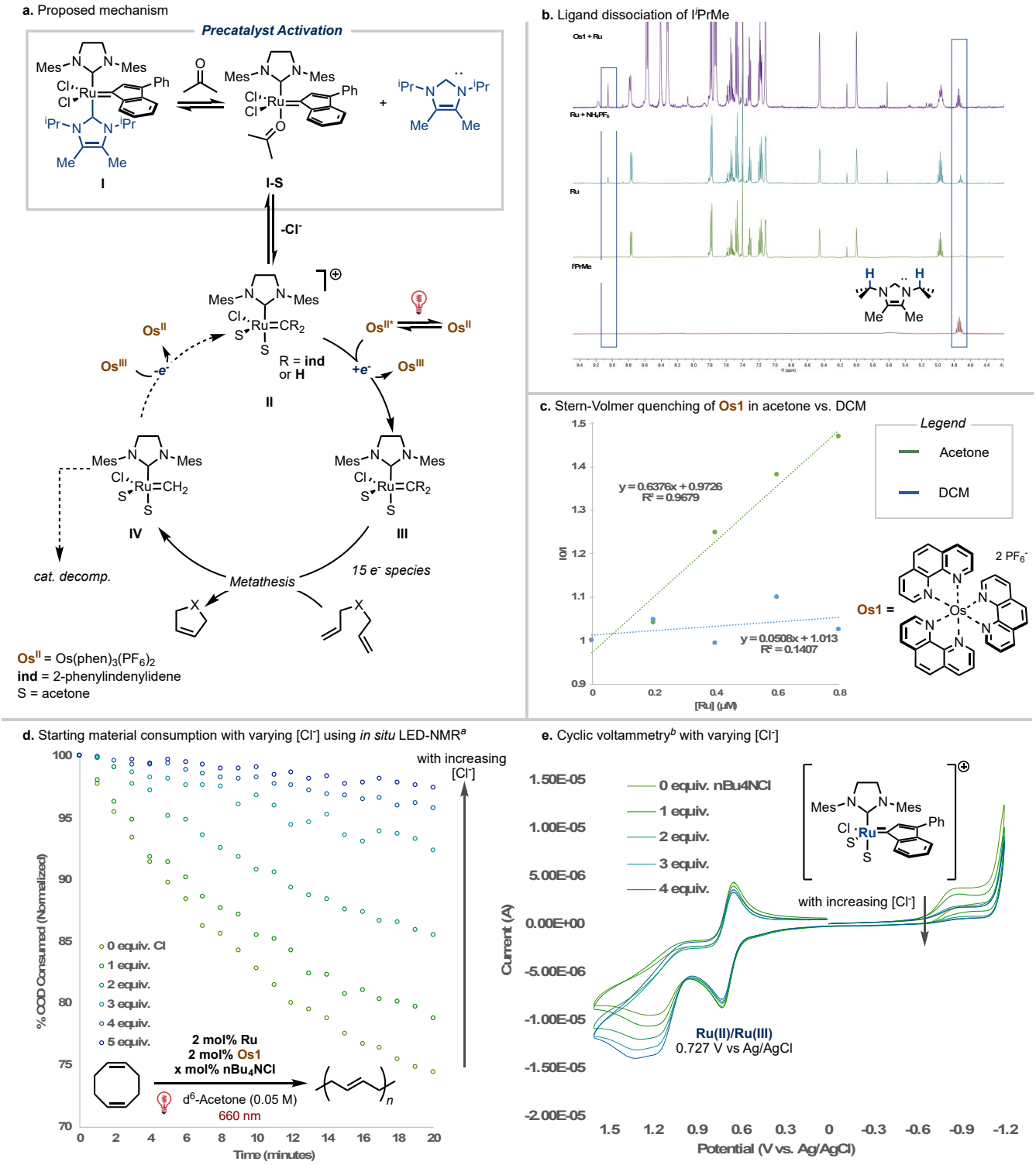

[a] Tracked by ^{1}H-NMR with mesitylene as internal standard. [b] Cyclic voltammetry: 3x10^{-3} M **Ru** in 0.1 M ^{n}Bu$_4$NPF$_6$ in acetone. Ag/AgCl reference electrode, glassy carbon working electrode. Pt counter electrode. * equiv. ^{n}Bu$_4$NCl relative to [Ru]

The Ru complex was then analyzed *via* cyclic voltammetry (CV), where we recognized an irreversible reductive wave at E_h = -0.85 V vs Ag/AgCl (SI Figure S3a). Here, we find that the rapid increase in intensity of the wave between -0.70 and -0.75 V vs. Ag/AgCl accounts for the difference in yields between **Os3** and **Os4**. With this in mind, we focused on how the catalyst is activated, starting with probing ligand dissociation. We hypothesized that the I^{i}PrMe carbene dissociates preferentially, consistent with literature precedent.[2]

The free ligand[22] is observed by ^{1}H-NMR when the Ru catalyst is mixed with the photocatalyst and when the catalyst is mixed with ^{n}Bu$_4$NPF$_6$ in the dark in d^6-acetone (Scheme 2b). This indicates that NHC dissociation event is fast and does not need an excited state Os photocatalyst.[23] However, while there is a slight increase in conversion when exogenous PF_6^- salt is added (Table 2, entries 4 and 5), the reaction still needs the Os photocatalyst, as no reactivity is observed in the presence of ^{n}Bu$_4$NPF$_6$ alone (Table 2, entry 2). The addition of 10 mol% free carbene to the reaction completely arrests metathesis, suggesting that dissociation of I^{i}PrMe is still an essential step in the activation of the complex (Table 2, entry 6). Thus, we hypothesize that the observed NHC dissociation event is required but not sufficient for reactivity.

However, we ascertain that the role of the solvent is two-fold in precatalyst activation: 1) aiding the dissociation of the NHC whilst maintaining metathesis latency *via* coordination, and 2) as a polar, ionizing environment. The improved reactivity with dilution most likely points to the increased ionization of the Ru precatalyst to its *cationic* complex, which we believe is the resting intermediate that is activated by the excited state Os photocatalyst. Cationic Ru(II) indenylidine complexes for metathesis have been reported and require high temperatures to activation;[24] herein, we show a mild activation strategy through a redox process. Stern-Volmer quenching studies of the Os photocatalyst were conducted in both DCM and acetone (Scheme 2c). The Ru complex only quenches the Os excited state in acetone, but not in DCM, corroborating that the solvent is important in the reaction mechanism. With evidence of the roles of the NHC and solvent in hand, we thus suggest rapid NHC dissociation (Scheme 2a, **I-S**) and catalyst ionization to generate the cationic intermediate **II** *in situ*, the proposed quencher for the excited state Os photocatalyst, whereupon single electron reduction would lead to the active species **III**. Further evidence pertaining to this will be discussed in greater detail.

Extending the electrochemical window in our cyclic voltammetry studies, we observe two waves at the reductive pass, the aforementioned E_h = -0.85 V vs Ag/AgCl and another wave at E_h = -1.18 V vs Ag/AgCl in acetone (SI Figure S3b). Comparing the CVs of Grubbs' II and its phenyl-indenylidene congener, we assign an irreversible wave at -1.00 V vs Ag/AgCl as the reduction of the indenylidene moiety (SI Figure S4); however, this reduction is too far to be reached by the photocatalysts. This indicates that the Os photocatalyst is not reducing the parent complex but a different species. As such, we hypothesized that the E_h = -0.85 V vs Ag/AgCl wave is the aforementioned cationic complex generated *in situ*. With this in mind, time studies for the ring opening of 1,5-cyclooctadiene (COD) were performed. Using LED-illuminated NMR spectroscopy,[25] we measured the starting material consumption for the ring opening of COD at different chloride concentrations. It was observed that the reaction rate decreases as the concentration of chloride increases, supporting of our hypothesized cationic complex mechanism (Scheme 2d). This salient intermediate is further corroborated by CV studies, where doping in ^{n}Bu$_4$NCl results in a decrease in intensity of the aforementioned irreversible wave at -0.85 V vs Ag/AgCl (Scheme 2e).

We further sought to determine the mechanism of deactivation. As depicted in Scheme 2a, there are two pathways through which **IV** can proceed to arrest metathesis: 1) back electron transfer from **IV** to oxidized Os catalyst regenerates **II**, or 2) a decomposition event occurs to remove the Ru from the catalytic cycle suggesting that only a minute amount of the catalyst is activated and performs metathesis until it reaches its turnover number - new initiators can only be activated when the light is on (i.e., slow activation).

Table 3: Analysis for slow activation of Ru catalyst

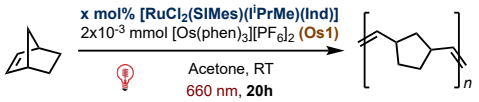

Entry	NBE:Os:Ru	% Conversion	Theo. M_n (kDa)	Exp M_n (kDa)*	Đ
1	500:1:1	58	27	6	5.38
2	500:1:0.1	74	348	19	3.58
3	500:1:0.01	34	1600	26	2.98
4	50:1:0.01	50	235	25	2.17
5	5:1:0.01	72	34	22	1.00

* Determined by GPC analysis.

First, we find that similar molecular weight polymers are obtained at exceedingly low Ru loadings, reaching around 25 kDa or approximately 250 units, suggesting slow initiation as a plausible mechanism. To deconvolute the rate of activation for the Ru catalyst, the ratio of Os to Ru was varied at high monomer loadings. Here, we use the polydispersity index (Đ) as the read out, expecting broad dispersities for a system where propagation is much faster than initiation. Expectedly, we then found a decrease in Đ with increasing [Os]:[Ru] (Table 3, Entries 1-3). This suggests that the excited state Os may be inefficient at activating the Ru catalyst, so higher Os loadings are required to provide an increased concentration of the active Ru species **III**.

Figure 1: Mechanism of polymerization

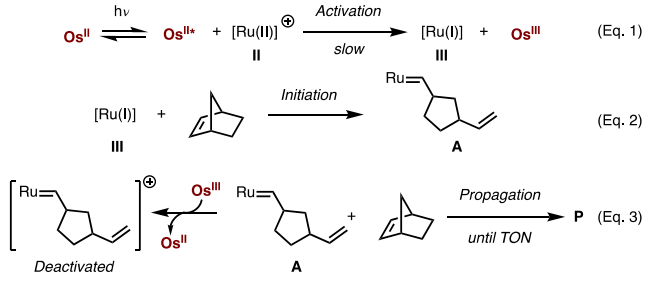

Then, the effect of monomer loading was studied (Table 3, Entries 3-5), where Đ narrows at decreased monomer concentrations. At high monomer loadings, we predict a steady state of the propagating intermediate **A** (Figure 1, Eq. 2). The rate of propagation is expectedly much faster than initiation, yielding a non-living system under these conditions. Therefore, when the monomer loading is decreased (Table 3, Entry 4-5), the rate of initiation is now competitive with the rate of propagation. As such, when decreasing the monomer loading, the polydispersity narrows to unity (Table 3, Entry 5). With this mechanistic hypothesis in mind, we suspect that a small number of initiators are activated at standard conditions (1:1 Os:Ru) and eventually reach their finite lifetimes when irradiation is halted. This

explains (1) the need for relatively high catalyst loading in RCM reactions and (2) the high polydispersity of the resulting polymers, i.e. the slow initiation of the Ru complex as a consequence of inefficient Os activation results in the formation of several active species **A** at different points in time, leading to different dispersities of polymers as the starting material is consumed and as the Ru catalyst eventually terminates. As a tentative mechanism, the solvent can act as a deactivator, as it is known that generated enolates (perhaps through NHC deprotonation of acetone) may decompose the metallacyclobutane intermediate and lead to catalyst decomposition.[26,27]

Scheme 3: Temporal control and barrier penetration

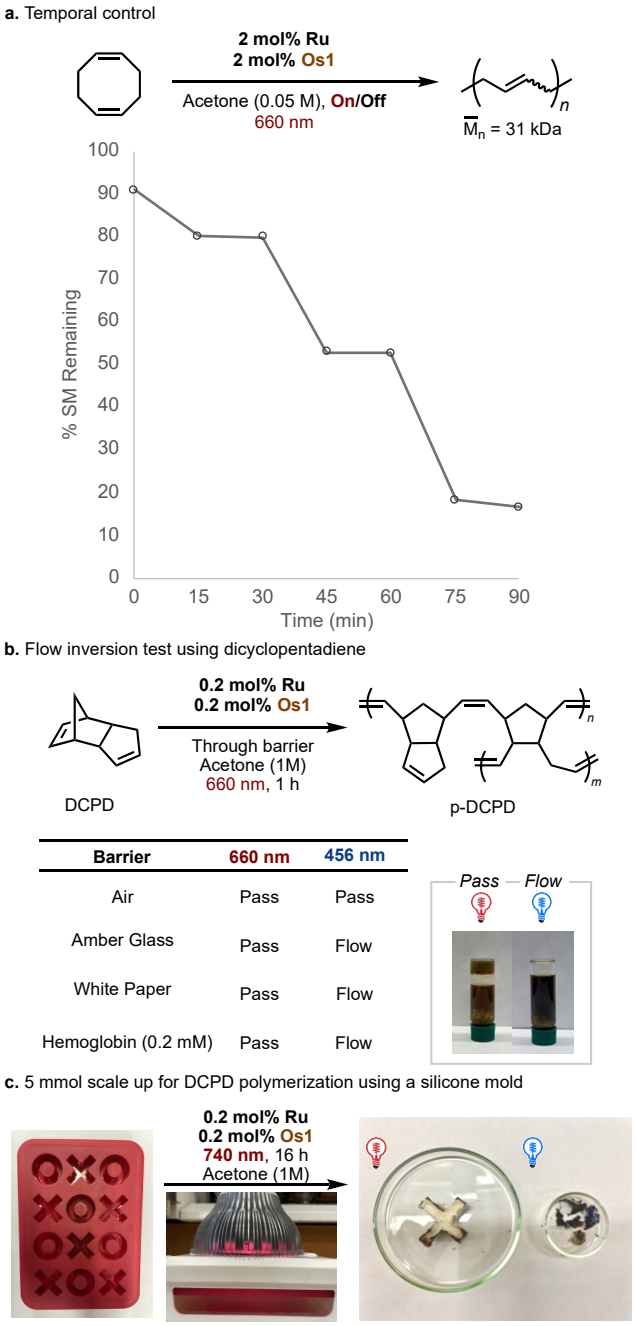

Finally, applications of our NIR system to polymerization were studied. Herein, we demonstrate spatiotemporal control of metathesis with NIR light as well as the added advantage of polymerization through barriers, which could be used as an orthogonal, controllable method to shaping dicyclopentadiene (DCPD) polymers compared to high temperature and pressure reaction injection molding. Due to the thermal reactivity of typical ruthenium catalysts, high levels of temporal control can be difficult. However, by virtue of its mechanism to photoactivation, reactivity is still expected to be completely arrested in periods without irradiation. Trace reactivity is often observed at Off periods as the complex equilibrates to its latent state. An On/Off study for the ring opening of COD was conducted. Excellent temporal control of starting material consumption is observed, with complete arrest of consumption during the off periods (Scheme 3a). GPC traces were obtained at each time point, where a bimodal distribution is observed (presumably a crosslink). Consistent with our mechanistic hypothesis, the COD polymer does not grow upon the On/Off periods, averaging at around 31 kDa at each time point, i.e. activation is light-controlled but propagation is not. Expectedly, slight growth of the larger polymer is observed and eventually reaches 120 kDa polymers, albeit in an uncontrolled fashion (SI Figure S7).

The ROMP of DCPD is also demonstrated to be spatially controlled using light, by moving a laser in a circular motion to draw a ring (SI Figure S2). Although other wavelengths of light can theoretically provide such spatiotemporal control of our system (as the Osmium photocatalyst can be activated from NIR to blue light), NIR light can penetrate through materials that lower wavelengths of light cannot, including biological tissue and Hemoglobin. Using this property of NIR light, we subjected the polymerization and crosslinking of DCPD through several barrier penetration tests (Scheme 3a). This was demonstrated through a simple flow inversion test where we expected a free-standing crosslinked material, given the reaction occurred through the barrier. Through amber glass, white paper, and a solution of Hemoglobin, free-standing poly-DCPD are observed when using NIR light (see picture), but not with blue light. A larger scale polymerization was achieved by shining light onto a mold covered with a silicone pad (Scheme 3b). The resulting polymers were shaped by the mold itself, indicating that the light had penetrated through the pad and initiated polymerization. Polymerization through the mold was attempted using blue light, which resulted in a thin film (no polymerization), while NIR light resulted in a 1 cm thick polymer in the shape of the mold. This shows that the NIR system is applicable for though-barrier polymer setting, a feature that cannot be accomplished using visible light methods.

CONCLUSION AND OUTLOOK

We have developed a NIR light-controlled Ru catalyzed olefin metathesis reaction with applications in polymerization. This system not only offers spatiotemporal control for the catalyzed metathesis reaction, but also provides all advantages of NIR light over blue light regarding barrier penetration, allowing for new ways to mold robust polymers. We also provide a series of mechanistic experiments that shed light on the underlying mechanism, which may pave new directions in designing and activating metathesis catalysts through novel, photoredox and/or electrochemical methods.

ASSOCIATED CONTENT

AUTHOR INFORMATION

Corresponding Author

* tr2504@columbia.edu

Author Contributions

The manuscript was written through contributions of all authors.

Funding Sources

For work conducted in Ghent, BOF grants and the iBOF C^3 projects to CSJC and SPN are gratefully acknowledged. Work conducted in New York was supported by the National Science Foundation. The authors acknowledge the use of facilities and instrumentation supported by NSF through the Columbia University, Columbia Nano Initiative, and the Materials Research Science and Engineering Center DMR-2011738.

Notes

A provisional patent has been filed on this work.

Supporting Information

Experimental procedures and characterization. The Supporting Information is available free of charge on the ACS Publications website.

ACKNOWLEDGMENT

We thank the National Science Foundation for support. We thank Adam Johns and Philip Wheeler (Umicore) for helpful discussions. We thank Dr. Philippe Chow for his help with polymer analysis. Ms Sofie Vanden Broeck (UGent) is gratefully acknowledged for technical assistance.

REFERENCES

(1) Ogba, O. M.; Warner, N. C.; O'Leary, D. J.; Grubbs, R. H. Recent Advances in Ruthenium-Based Olefin Metathesis. *Chem. Soc. Rev.* **2018**, *47* (12), 4510-4544.

(2) César, V.; Lavigne, G. Olefin Metathesis: Theory and Practice. Edited by Karol Grela. *Angew. Chem. Int. Ed.* **2015**, *54* (13), 3856–3857.

(3) Grubbs, R. H.; Love, J.A. *Handbook of Metathesis*, Wiley-VCH, Weinheim, Germany, **2003**, 296-319.

(4) Higman, C. S.; Lummiss, J. A. M.; Fogg, D. E. Olefin Metathesis at the Dawn of Implementation in Pharmaceutical and Specialty-Chemicals Manufacturing. *Angew. Chem. Int. Ed.* **2016**, *55* (11), 3552–3565.

(5) Leitgeb, A.; Wappel, J.; Slugovc, C. The ROMP Toolbox Upgraded. *Polymer* **2010**, *51* (14), 2927-2946.

(6) Hejl, A.; Scherman, O. A.; Grubbs, R. H. Ring-Opening Metathesis Polymerization of Functionalized Low-Strain Monomers with Ruthenium-Based Catalysts. *Macromolecules* **2005**, *38* (17), 7214-7218.

(7) Naumann, S.; Buchmeiser, M. R. Latent and Delayed Action Polymerization Systems. *Macromol. Rapid Commun.* **2014**, *35* (7), 682–701.

(8) Doerr, A. M.; Burroughs, J. M.; Gitter, S. R.; Yang, X.; Boydston, A. J.; Long, B. K. Advances in Polymerizations Modulated by External Stimuli. *ACS Catal.* **2020**, *10* (24), 14457–14515.

(9) Varnado, C. D.; Jr; Rosen, E. L.; Collins, M. S.; Lynch, V. M.; Bielawski, C. W. Synthesis and Study of Olefin Metathesis Catalysts Supported by Redox-Switchable Diaminocarbene[3]Ferrocenophanes. *Dalton Trans.* **2013**, *42* (36), 13251–13264.

(10) El-Shahawi, M. S.; Shoair, A. F. Synthesis, Spectroscopic Characterization, Redox Properties and Catalytic Activity of Some Ruthenium(II) Complexes Containing Aromatic Aldehyde and Triphenylphosphine or Triphenylarsine. *Spectrochim. Acta. A. Mol. Biomol. Spectrosc.* **2004**, *60* (1), 121–127.

(11) Ahumada, G.; Ryu, Y.; Bielawski, C. W. Potentiostatically Controlled Olefin Metathesis. *Organometallics* **2020**, *39* (10), 1744–1750.

(12) Piermattei, A.; Karthikeyan, S.; Sijbesma, R. P. Activating Catalysts with Mechanical Force. *Nat. Chem.* **2009**, *1* (2), 133–137.

(13) Vidavsky, Y.; Lemcoff, N. G. Light-Induced Olefin Metathesis. *Beilstein J. Org. Chem.* **2010**, *6* (1), 1106–1119.

(14) Keitz, B. K.; Grubbs, R. H. A Tandem Approach to Photoactivated Olefin Metathesis: Combining a Photoacid Generator with an Acid Activated Catalyst. *J. Am. Chem. Soc.* **2009**, *131* (6), 2038–2039.

(15) Eivgi, O.; Vaisman, A.; Lemcoff, N. G. Latent, Yet Highly Active Photoswitchable Olefin Metathesis Precatalysts Bearing Cyclic Alkyl Amino Carbene (CAAC)/Phosphite Ligands. *ACS Catal.* **2021**, *11* (2), 703–709.

(16) Nechmad, N. B.; Lemcoff, N. G. Sulfur-Chelated Ruthenium Olefin Metathesis Catalysts. *Synlett* **2021**, *32* (03), 258-266.

(17) Ogawa, K. A.; Goetz, A. E.; Boydston, A. J. Metal-Free Ring-Opening Metathesis Polymerization. *J. Am. Chem. Soc.* **2015**, *137* (4), 1400–1403.

(18) Theunissen, C.; Ashley, M. A.; Rovis, T. Visible-Light-Controlled Ruthenium-Catalyzed Olefin Metathesis. *J. Am. Chem. Soc.* **2019**, *141* (17), 6791–6796.

(19) Bantreil, X.; Randall, R. A. M.; Slawin, A. M. Z.; Nolan, S. P. Ruthenium Complexes Bearing Two N-Heterocyclic Carbene Ligands in Low Catalyst Loading Olefin Metathesis Reactions. *Organometallics* **2010**, *29* (13), 3007–3011.

(20) a) Ravetz, B. D.; Tay, N. E. S.; Joe, C. L.; Sezen-Edmonds, M.; Schmidt, M. A.; Tan, Y.; Janey, J. M.; Eastgate, M. D.; Rovis, T. Development of a Platform for Near-Infrared Photoredox Catalysis. *ACS Cent. Sci.* **2020**, *6* (11), 2053–2059. b) Goldschmid, S. L.; Bednárová, E.; Beck, L. R.; Xie, K.; Tay, N. E. S.; Ravetz, B. D.; Li, J.; Joe, C. L.; Rovis, T. Tuning the Electrochemical and Photophysical Properties of Osmium-Based Photoredox Catalysts. *Synlett* **2022**, *33*, 247-258.

(21) Goldschmid, S. L.; Soon Tay, N. E.; Joe, C. L.; Lainhart, B. C.; Sherwood, T. C.; Simmons, E. M.; Sezen-Edmonds, M.; Rovis, T. Overcoming Photochemical Limitations in Metallaphotoredox Catalysis: Red-Light-Driven C-N Cross-Coupling. *J. Am. Chem. Soc.* **2022**, *144* (49), 22409-22415.

(22) I^iPrMe was synthesized as described in Kuhn, N.; Kratz, T. Synthesis of Imidazol-2-Ylidenes by Reduction of Imidazole-2(3H)-Thiones. *Synthesis* **1993**, *1993* (6), 561–562.

(23) We propose that the salt facilitates the deprotonation of acetone (pKa = 26 in DMSO) by the free NHC (pKa = 24 in DMSO). This deprotonation was probed by stirring the free NHC in acetone, where the protonated NHC and the aldol product of acetone is observed only when nBu_4NPF_6 or $[Os(phen)_3][PF_6]_2$ is added. For the pKa of the NHC, see: Alder, R. W.; Allen, P. R.; Williams, S. J. Stable Carbenes as Strong Bases. *J. Chem. Soc. Chem. Commun.* **1995**, *12*, 1267–1268.

(24) Songis, O.; Slawin, A. M. Z.; Cazin, C. S. J. An Unusual Cationic Ru(II) Indenylidene Complex and Its Ru(III) Derivative—Efficient Catalysts for High Temperature Olefin Metathesis Reactions. *Chem. Commun.* **2012**, *48* (9), 1266–1268.

(25) Ji, Y.; DiRocco, D. A.; Hong, C. M.; Wismer, M. K.; Reibarkh, M. Facile Quantum Yield Determination via NMR Actinometry. *Org. Lett.* **2018**, *20* (8), 2156–2159.

(26) Bailey, G. A; Lummiss, J. A. M.; Foscato, M.; Occhipinti, G.; McDonald, R.; Jensen, V. R.; Fogg, D. E. Decomposition of Olefin Metathesis Catalysts by Brønsted Base: Metallacyclobutane Deprotonation as a Primary Deactivating Event. *J. Am. Chem. Soc.* **2017**, *139* (46), 16446-16449.

(27) For a review on Decomposition of Olefin Metathesis Catalysts, see: Jawiczuk, M.; Marczyk, A.; Trzaskowski, B. Decomposition of Ruthenium Olefin Metathesis Catalyst. *Catalysts* **2020**, *10* (8), 887.

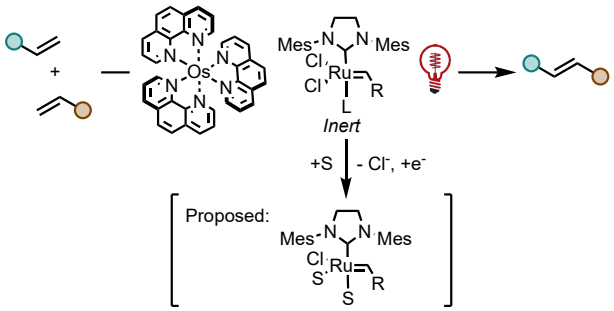
Mes
Cl
Cl
Ru
R
L
Inert
+S
- Cl-, +e-
Proposed:
Mes
Cl
S
Ru
R
S